Thermal Advances 6 (2026) 100096

Contents lists available at ScienceDirect

Thermal Advances

journal homepage: www.elsevier.com/locate/thradv

Full Length Article

Pigment power: a comparative study on the effect of different cadmium sulfide pigments on the curing of polyunsaturated drying oils

Giulia Caroti [a], Silvia Pizzimenti [b,*], Rafaella Georgiou [a,c], Marta Ghirardello [d], Rita Carosi [a], Emma Cantisani [e], Ilaria Bonaduce [a], Daniela Comelli [d], Celia Duce [a]

[a] Department of Chemistry and Industrial Chemistry, University of Pisa, Pisa, 56124, Italy
[b] Department of Chemical Sciences, Università of Naples "Federico II", 80126, Naples, Italy
[c] Department of Physics, University of Wisconsin-Madison, 53706 Madison, Wisconsin, US
[d] Department of Physics, Politecnico di Milano, 20133, Milan, Italy
[e] CNR-ISPC-Institute of Heritage Science (Florence unit), 50019, Sesto Fiorentino, Florence, Italy

ARTICLE INFO

Keywords:
Oil paint
Cadmium sulphide
Cadmium sulphoselenide
Cadium selenide
Oil curing
Polymerisation
Oxidative degradation, Polyunsaturated drying oils

ABSTRACT

The present study investigates the effects of various cadmium-based pigments on the curing behaviour of linseed oil. Model linseed oil paints, prepared starting from different cadmium yellow pigments, were subjected to accelerated aging inside a thermobalance at 80 °C, under oxygen flow and in the dark. Thermogravimetric analysis (TGA) was used to monitor the mass change of the paint samples induced by oil autoxidation during curing, while ATR-FTIR spectroscopy provided insights into molecular transformations before and after thermal exposure. Results reveal that cadmium yellow pigments with identical chemical composition (CdS) can induce different curing kinetics, depending on the crystalline features of the pigments, namely crystallite size and degree of crystallinity. Pigments having nanocrystalline structures delayed the onset of peroxide propagation, resulting in extended induction times and incomplete polymer network formation in the timeframe investigated. These paints also showed formation of cadmium carboxylates and cadmium sulphates. These results may be related to the intrinsic peroxidase-like (POD-like) catalytic activity of nanocrystalline CdS, reported here for the first time in a non-aqueous medium.

1. Introduction

Oil paint is a composite material made of pigment particles dispersed in a drying oil. After application, the oil undergoes a slow curing process driven by autoxidation, a complex sequence of reactions in which unsaturated fatty acids react with atmospheric oxygen. During curing, two competing processes occur simultaneously: oxidative degradation and polymerization (cross-linking). Cross-linking leads to the formation of a solid, cohesive polymer network, whereas oxidative degradation results in chain scission and the formation of low-molecular-weight products [1]. Since cross-linking and oxidative degradation are concomitant processes that determine the characteristics of the evolving polymer network in a curing drying oil, understanding their relative contribution is crucial for predicting and controlling the final properties of oil-based paint layer[2–5].

In the case of oils alone, a high content of bis-allylic hydrogens, as found in linseed oil, promotes cross-linking, whereas oils with a lower (e.g., safflower oil) or negligible (e.g., olive oil) bis-allylic content are progressively more susceptible to oxidative degradation[2].

For a given oil, multiple factors can influence the curing pathway, favouring either oxidative degradation or polymerization. These factors include the pigment to the presence of co-binders such as protein-based materials[6], variations in the in the paint preparation method[6], the addition of metal-based driers[5,7–8], the environmental conditions [9], binder ratio [10], as well as the type and properties of the pigment used[3–4,11–16], For example, when lead white is mixed with linseed or safflower oil, the resulting paint forms a well cross-linked polymer network within a relatively short period of time. In contrast, ultramarine blue exhibits markedly different behaviour, particularly when combined with a semi-drying oil (safflower oil). Ultramarine blue promotes oxidative degradation of the binder, which may explain the documented degradation issues associated with ultramarine blue paint layers, such as loss of cohesion of the binder and water sensitivity of the paint layers[4]. Carbon black shows a strong antioxidant effect, slowing down

* Corresponding author.
E-mail address: silvia.pizzimenti@unina.it (S. Pizzimenti).

https://doi.org/10.1016/j.thradv.2026.100096

Available online 10 January 2026
3050-4635/© 2026 The Authors. Published by Elsevier B.V. This is an open access article under the CC BY-NC-ND license (http://creativecommons.org/licenses/by-nc-nd/4.0/).

Table 1
Pigments name, source (commercial or synthesized) and features according to XRD analysis: chemical formula, hexagonal form content (H), type phase present (phase) and crystallite size.

Pigment name	Commercial/synthesized	Chemical formula	H	Phase	Crystallite size (nm)	notes	Reference
W&N1	Synthesized – historical synthesis method	CdS	0.79	α + β	21	Polytype crystal structure	[39]
W&N6	Synthesized – historical synthesis method	CdS	0.45	α + β	32	Polytype crystal structure	[39]
Y3	Synthesized – historical synthesis method	CdS	0	β	3	poorly crystalline cub CdS	[39]
Y5	Synthesized – historical synthesis method	CdS	0	β	3	poorly crystalline cub CdS	[39]
Y9	Synthesized – historical synthesis method	CdS	0	β	3	poorly crystalline cub CdS	[39]
CUB	Synthesized –synthesis method	CdS	0.17	β	24	Polytype crystal structure	[39]
HEX	Synthesized –synthesis method	CdS	1	α	98	Greenockite CdO (trace)	[39]
KP4	Commercial: Kremer Pigmente, Cadmium yellow dark #21060	CdS	0.92	α	58	Greenockite and barite ($BaSO_4$)	[39]
$CdS_{1-x}Se_x$	Commercial: Golden Artist Color, PR108 (77202)	$CdS_{(0.72)}Se_{(0.28)}$	1	α	54		
CdSe	Commercial: Sigma Aldrich	CdSe	1	α	61		

unsaturated moieties consumption and peroxides formation in linseed oil based paints, thus accounting for the well-known delayed drying of paint layers containing this pigment. Carbon black also inhibits radical chain propagation and competitive oxidative degradation reactions[3].

Among the wide variety of pigments introduced in the 19th and 20th centuries, cadmium yellow (CdY), a family of cadmium sulfide (CdS) pigments, was particularly appreciated by renewed artists, including Picasso, Matisse, Van Gogh, Munch and Mirò for their vibrant colours and outstanding coverage [17–23]. This class of pigments was first produced in 1910 via calcination of cadmium sulphide, selenium, and sulphur, with a subsequent synthesis route introduced in 1919 involving precipitation from alkaline solutions and heat treatment to obtain the red form[24].

CdS belongs to IIb-IVa direct band gap semiconductor group[25]. It is characterized by a direct and large band gap at room temperature of 2.4 eV (516 nm) for the hexagonal crystal structure and 2.3 eV (539 nm) for the cubic one. The band gap shifts toward higher energy values when zinc is introduced in CdS crystal lattice to form the solid solution $Cd_{1-x}Zn_xS$ (up to 3.6 eV - 344 nm). Vice versa, when Se is introduced as the substitutional ion ($CdS_{1-x}Se_x$) the band gap decreases until 1.8 eV (570 nm).

CdS has been extensively studied in the literature for its optical properties, which are tunable by changing the size and shape of it crystals[26], showing potential applications in photovoltaic devices, as photocatalysts, sensors, and quantum dots[27–28]. Indeed, CdS nanoparticles and nanocrystals exhibit peculiar electronic and optical properties and show photocatalytic activity and an intrinsic peroxidase-like (POD-like) catalytic activity[26,29] in aqueous solutions. For these reason they are called inorganic enzymes [26,29]. These two catalytic activities have been thoroughly studied in literature and exploited for biosensing, remediation of waste waters and oxidations of organic pollutants [26,29]. Peroxidases catalyse the reduction of peroxides and hydroperoxides to alcohols and water and the simultaneous oxidation of an organic molecule present in the same aqueous solution.

It is well documented that CdS can undergo photooxidation reactions [30] when mixed with oil in oil-based paintings. Observed degradation phenomena in paints include colour changes, loss of surface gloss, chalking, flaking, crumbling, spalling, embrittlement of the paint, and the formation of superficial crusts[17–22]. The main degradation products are cadmium sulfate or hydrated cadmium sulphate, but other cadmium species, such as cadmium oxalate and cadmium carbonates are also detected[18,22].

The influence of environmental conditions on the tendency of CdY paints to degrade was investigated by Monico et al., [30–31] through the study of model paint systems, composed of hexagonal and cubic CdS, $Cd_{1-x}Zn_xS$ and $CdS_{1-x}Se_x$ pigments dispersed in linseed oil. Following artificial aging of the paint layers, exposed to UV light and elevated relative humidity, a mechanism for the photo-oxidation of CdY paints was proposed. Upon illumination with supra band gap light, the pigment generates electron-hole pairs ($e^- + h^+$), which can recombine dissipating the adsorbed light energy as heat or migrate to the surface of the particles. The hole migrated to the surface can interact with the organic binder but also with the particle itself. So, the photocatalytic degradative oxidation of the oil occurs as a competitive phenomenon compared to the photocorrosion of CdS.

Surface defects, acting as charge traps, can further enhance CdS reactivity and impact the paint stability[32]. Previous works by Comelli *et al.* [17] and Ghirardello *et al.*[33] investigated in detail the role of crystalline defects in the degradation of CdY paints, using photoluminescence emission analysis. These studies were prompted by the discovery of two CdY paints in a Picasso painting that, despite having the same chemical composition and having been exposed to the same environmental conditions for years, showed markedly different states of conservation. One paint remained intact, retaining its bright yellow color, while the other had degraded, turning brownish and exhibiting increased fragility due to the degradation of its organic components. Time-gated photoluminescence spectroscopy revealed that the degraded paint exhibited an optical emission from trap states that is twenty times more intense than that observed in the intact paint. Moreover, the emission from trap states in the degraded paint is shifted to shorter wavelengths. Both observations point to the presence of highly defective CdS nanoparticles[34]. The authors therefore speculated that the degraded paints contain nanocrystalline CdS, similar to what has been reported in other degraded CdY paints[35]. The large surface-to-volume ratio of CdS nanoparticles makes them highly reactive and less stable [36], contributing significantly to the degradation of the paint [17,33].

It is also important to consider that residues from the synthesis can still be contained in the pigment and can influence the chemical stability of it. Mayda et al.[37] showed that the presence of Cd(OH)Cl, a residue of the wet synthesis route, can act as an oxidative catalyst for the formation of $CdSO_4$.

Although CdY pigments are recognized as photocatalysts for oil oxidation, the curing process of paint films remains significantly slow[5, 38]. Indeed, commercial formulations typically include driers to reduce the drying time[5].

This study aims to investigate the early stage of curing, the curing kinetic and the formation of the polymer network of linseed oil in the presence of various CdY pigments. In particular, we investigated if the well-known slow curing kinetics of Cd-based oil paints[5] can potentially influence the early curing stages and the balance between polymerization and oxidative degradation of the oil binder. Model linseed oil paints, prepared starting from different cadmium yellow pigments, were subjected to accelerated aging. Experiments were carried under controlled environmental conditions and in the dark, to exclude any contribution from their photocatalytic activity. The CdY pigments selected for the present study differ in the historical synthesis method, their crystalline forms, physical properties, and degrees of crystallinity. For comparison, model paints made with commercial CdS, $CdS_{1-x}Se_x$ and

CdSe were also examined.

To this aim, we applied a validated methodological approach to assess the relative contributions of polymerization and oxidative degradation during the autoxidation of oils[2]. This method is based on the acquisition of constant-temperature oxygen uptake curves using thermogravimetric analysis (TGA) and their fitting with a semi-empirical equation. The method is applicable to both poly-unsaturated oils and oil paint systems[5].

For the purpose, paints made of the selected CdY pigments, were subjected to accelerated aging at 80 °C and the mass change was monitored by TGA with the samples kept in the dark throughout the measurement. Infrared spectra using attenuated total reflectance - Fourier transform infrared spectroscopy (ATR-FTIR) were obtained before and after TGA to evaluate changes in the spectral features of the oil oxidation upon accelerated curing.

2. Materials and methods

2.1. Pigments selection and characterization (XRD)

The selected CdY were synthetized on the base of different recipes, both modern and historical.

Referring to Table 1, those samples labelled as W&N series were synthetized on the basis of historical methods found in the W&N 19th c. archive database starting from different cadmium salts in aqueous solutions and hydrogen sulfide gas, as described in details in Ghirardello *et al*[11]. Samples belonging to the Y series were synthesized via a different historical method starting from different cadmium salts and sodium sulphide in aqueous solution[24]. Details on the synthesis procedure are provided in Supplementary Information. Reference CdS pigments in the cubic and hexagonal crystal structure (quoted as CUB and HEX samples) were synthesized via two ad-hoc synthesis methods [11]. Reference CdSe was purchased from Sigma Aldrich, reference commercial CdY pigment (KP4) was purchased from Kremer Pigmente, CdS. $CdS_{(0.72)}Se_{(0.28)}$ was kindly provided by Golden Artist Color,.

XRD analysis of pigments not already characterized in Ghirardello *et al.*, [39] were performed using an X'Pert Pro PANalytical copper anticathode diffractometer (λ=1.5406 Å). Diffraction patterns were acquired with a current of 30 mA and a voltage of 40 kV, exploring a 2θ angular range of 15° to 60°, with a scan step of 0.017° and a total acquisition time for each pattern of about 39 minutes. Identification of mineralogical phases and calculation of peak intensity were performed using X'Pert High Score software with the ICDD database. For CdS pigments the formulas reported in Ghirardello *et al.*[39] were used to calculate crystallite size and hexagonality (H).

To calculate crystallite size we used the Scherrer formula[40]:

$$D = \frac{0.9\ \lambda}{(\beta\ \cos\theta)}$$

where λ is the wavelength of the incident radiation, θ is the Bragg angle, and β is the FWHM (Full Width at Half Maximum) of the diffraction angle θ.

To calculate hexagonality (fraction of the hexagonal form H) we used equation proposed by [41]

$$H = \frac{4R}{(3R + 1.33)}$$

where R is given by the ratio

$$R = \frac{I(100)}{I(002) + I(111)}$$

in which $I_{(100)}$ represents the integrated intensities of the peak corresponding to α-CdS diffraction peak and $I_{(002)} + I_{(111)}$ the one of β-CdS + α-CdS diffraction peaks.

Table 2
Description of model paints prepared for the present study.

Model paint name	Pigment	Oil	Oil content (%)
W&N1	CdS	Linseed oil	33.4
W&N6	CdS	Linseed oil	29.9
Y3	CdS	Linseed oil	32.8
Y5	CdS	Linseed oil	32.7
Y9	CdS	Linseed oil	36.6
CUB	CdS	Linseed oil	28.6
HEX	CdS	Linseed oil	32.3
KP4	CdS	Linseed oil	32.6
CdSe	CdSe	Linseed oil	32.6
$CdS_{(0.72)}Se_{(0.28)}$	$CdS_{(0.72)}Se_{(0.28)}$	Linseed oil	27.6

While the crystallite sizes of $CdS_{(0.72)}$ $Se_{(0.28)}$ and CdSe were calculated in two different ways: i) from the diffraction of the same hkl 002 plane with respect to species containing αCdS (hexagonal) and βCdS (cubic) and 2) from other diffraction peaks of the hkl planes (100), (101), (110), (102).

Table 1 reports the mean of the values obtained. It is worth noting that selected pigments exhibit different crystalline characteristics, such as crystalline degree, size of the crystallite, and the relative content of hexagonal phase (Table 1).

2.2. Model paints preparation

A weighted amount of pigment was added to a weighted amount of oil and mixed thoroughly by means of a metallic spatula to create the model paint until a homogeneous paste was achieved. Refined linseed oil was purchased from Maimeri (product code: 5816650 - Olio di lino). Table 2 shows the model paints composition.

2.3. Artificial ageing and paint curing monitoring (TGA)

Isothermal TGA was carried with a TA-Instruments thermo-balance, model Q5000IR, under a constant dry airflow (25 mL·min^{-1}) at 80°C for 3000 min. The sample mass ranged between 9 and 11 mg. The thermogravimetric curves were normalized to the oil content in the sample. The fitting of the oxygen uptake curves was performed with the software OriginPro8.

The experimental data were fitted with a semi-empirical fitting equation (eq. 1)[2]:

$$mass\ \%(t) = \frac{Ae^{-\lambda_1 t} - B}{1 + e^{-\lambda_0 (t - t_0)}} + 100 \quad (1)$$

$\boldsymbol{A}$ represents the amount of mass which is lost by the paint due to oxidative degradation. $\boldsymbol{B}$ represents the deviation of the curve from 100 % for time t tending to infinity. $\boldsymbol{\lambda_0}$ is the apparent time constant related to the mass increase. $\boldsymbol{\lambda_1}$ is the time constants related to the mass loss. $\boldsymbol{t_0}$ is the time at the abscissa of the inflexion point of the sigmoidal function, which is related to the induction time of the oxygen uptake. To estimate the amount of oxygen taken up by the paint upon curing, parameter $\boldsymbol{C} = A_{corr} - B$ is calculated, where $A_{corr} = Ae^{-\lambda_1 t}$ represents the effective total mass loss. $\boldsymbol{A_{corr}}$ is calculated at $t = t_{onset}$, t_{onset} being the abscissa of the intersection point between the baseline and the tangent to the curve at the first inflexion point. t_{onset} was calculated by Python. Further details on the fitting equation and parameters are reported in [2].

2.4. Molecular features characterization (ATR-FTIR)

A Perkin-Elmer Frontiers FTIR Spectrophotometer, equipped with a universal attenuated total reflectance (ATR) accessory and a triglycine sulfate TGS detector was used to acquired infrared spectra. Spectra were recorded at 4 cm^{-1} resolution and 64 scans were recorded. Analyses were carried out in triplicates, one spectrum among the three was selected since the spectra showed reproducible spectral features. A straight

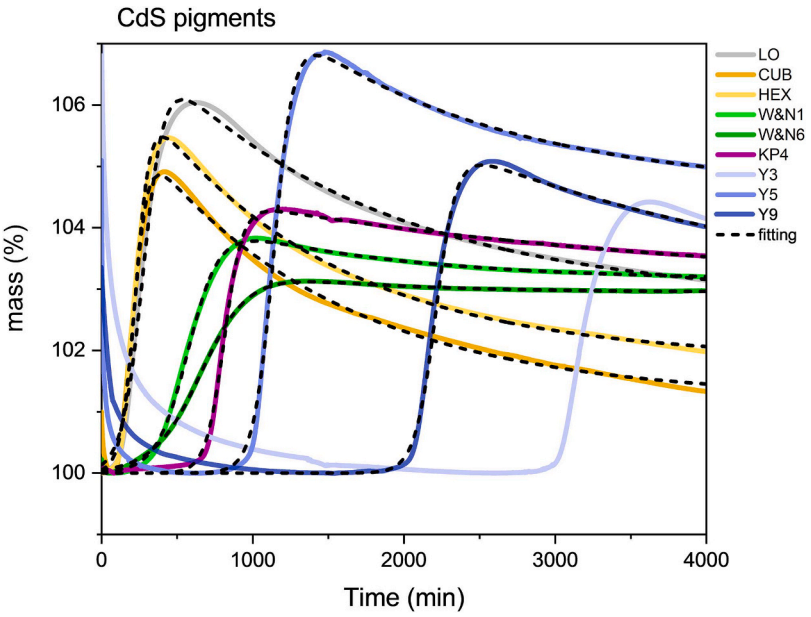

Fig. 1. Experimental (colored solid line) oxygen uptake obtained with TGA, and theoretical (black dash line) data as obtained by Eq. (1) of all CdS pigments. All data were normalized for the oil content. The oxygen uptake of linseed oil alone (LO) has been added as a reference material.

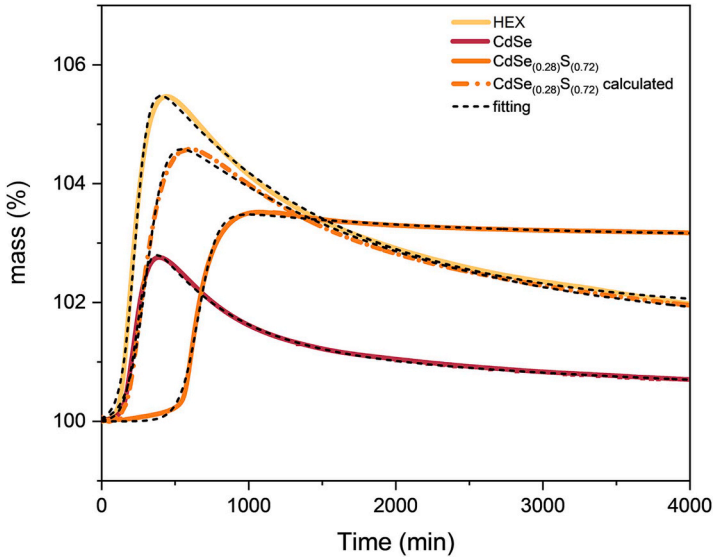

Fig. 2. Experimental (colored lines) oxygen uptake obtained with TGA, and theoretical (black dash line) data as obtained by Eq. (1) of paints made of CdS (HEX), CdSe, experimental and calculated $CdSe_{(0.28)}S_{(0.72)}$ based on the relative content of selenium (28 %) and sulphur (72 %). All data were normalized for the oil content.

baseline passing through the ordinates at 4000, 3700, 3035, 2500, 1900, 1790, 1500 and 850 cm^{-1} was subtracted with the"Spectrum" software (Pelkin Elmer), and the spectra were normalized in the 1470–1450 cm^{-1} region. Analyses were performed on the freshly prepared liquid paint and on the paint sample collected after the TGA analysis (scratched from the cup used during the analysis). Depending on the pigment, the paint after the TGA analysis appeared more or less dry.

3. Results and discussion

We produced model paints made of CdS pigments having different degrees of crystallinity, size of the crystallite, and relative content of hexagonal phase. Further, three paints, respectively made of $Cd_{(0.9)}Zn_{(0.1)}S$, $CdS_{(0.72)}Se_{(0.28)}$ and CdSe were also considered. Model paints were subjected to accelerated thermal aging by means of a thermogravimetric (TGA) analysis at 80°C for 4000 minutes. The analysis, hereafter referred to as "mass uptake," was used to monitor the change in sample mass due to reaction with oxygen during accelerated oil curing. The mass change presents two distinct regions. The first exhibits a mass increase and is followed by a mass loss that typically, but not always, stabilizes over time, into a plateau. The initial mass gain is primarily due to peroxide formation, whereas the subsequent mass loss results from oxidation driven chain scission – oxidative degradation - which produces volatile compounds that evaporate under the experimental conditions adopted. Oxidative degradation and cross-linking are competitive phenomena, and the observed mass change at any given moment represents the balance between the complex interplay between these two processes, as volatile compounds can evolve as soon as the initial peroxides begin to decompose. The amount of oxygen added to the sample is estimated by parameter *C*. The tendency toward oxidative

Table 3
Parameters χ^2 and R coefficients obtained by fitting the experimental oxygen uptake curves with Eq.1. Regarding the fitted parameters, for all samples analysed, the standard errors of parameters A and B parameter are equal or lower than 0.2 and 0.2, respectively. Standard errors of parameters λ_0, λ_1 are equal or lower than $4{\cdot}10^{-4}$ and $7{\cdot}10^{-2}$, respectively. Standard error of parameter t_0 is equal or lower than 6.9.

	t_0 (min)	t_{onset} (min)	A_{corr} (%)	B (%)	C (%)	$\lambda_0 \cdot 10^2$ (min^{-1})	$\lambda_1 \cdot 10^4$ (min^{-1})	χ[2]	R
LO	282.0	223.6	5.7	-2.8	8.5	1.4	6.6	0.009	0.994
W&N1	579.7	518.6	2.4	-3.1	5.5	1.0	8.1	9.71E-4	0.999
W&N6	671.2	648.6	2.1	-3.0	5.0	0.6	1.1	1.86E-4	0.999
Y5	1143.3	1106.2	13.5	-4.6	18.2	1.5	7.0	0.0507	0.997
Y9	2213.6	2197.4	14.2	-2.5	16.8	1.5	3.7	0.1173	0.973
CUB	219.1	177.8	5.8	-1.2	7.0	2.0	7.6	0.008	0.993
HEX	230.7	193.0	6.1	-1.9	7.9	2.1	8.0	0.004	0.997
KP4	813.3	784.7	2.4	-3.0	5.3	1.6	3.2	0.002	0.999
$CdSe_{(0.28)}S_{(0.72)}$	659.0	628.1	1.1	-3.1	4.3	1.5	6.7	0.002	0.999
$CdSe_{(0.28)}S_{(0.72)}$ calculated	311.1	259.7	5.1	-1.5	6.6	1.6	5.9	0.003	0.997
CdSe	237.3	221.7	4.1	-0.6	4.7	2.7	11.0	0.003	0.989

degradation can be evaluated from the effective total mass loss parameter A_{corr}: a higher value of A_{corr} suggests a higher tendency of the

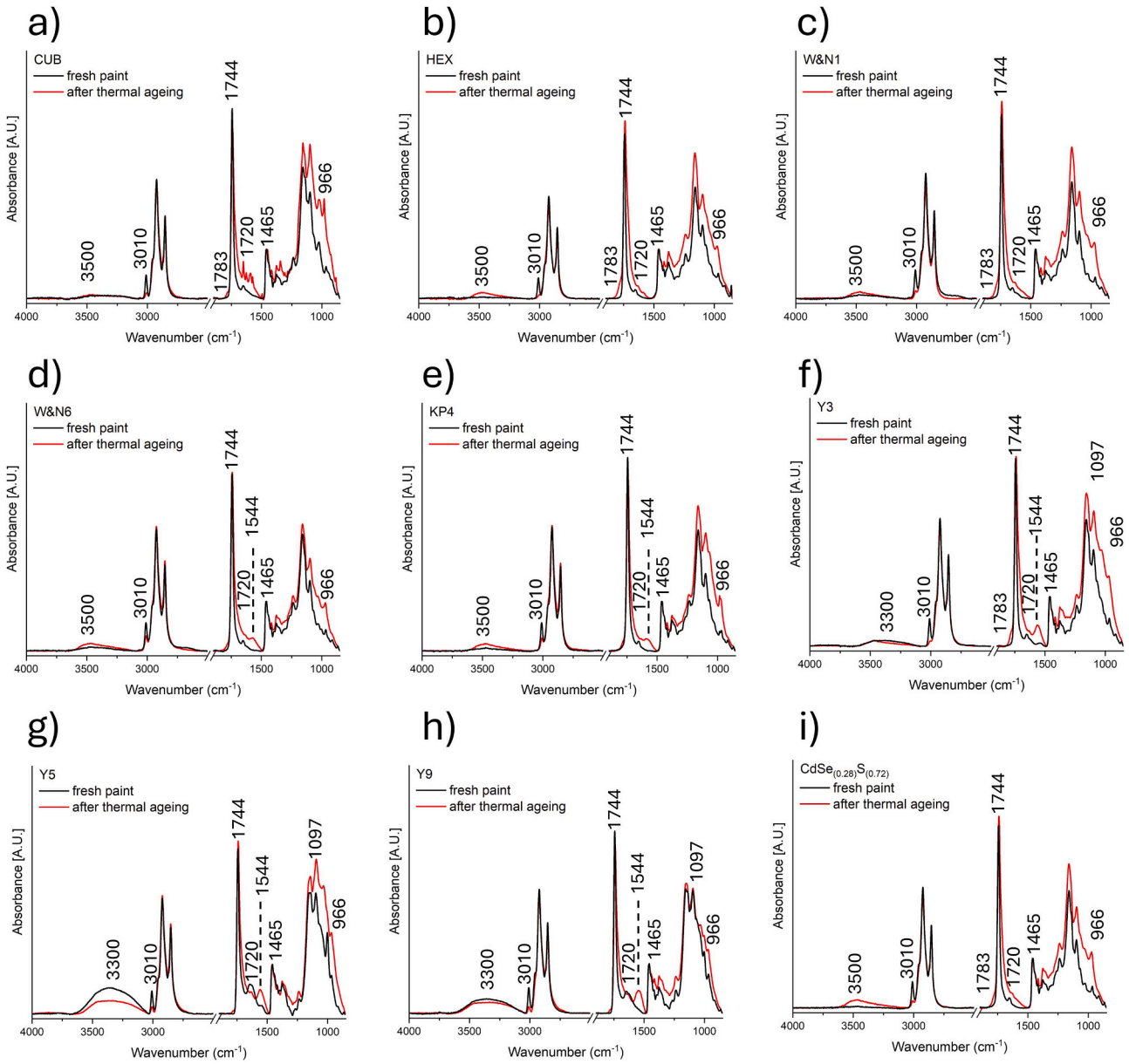

Fig. 3. ATR-FTIR spectra of the fresh paint before and after the thermal ageing carried out by TGA (80°C for 4000 minutes).

paint toward oxidative degradation during curing leading to the formation of a more polar film. A lower degree of oxidative degradation (lower values of A_{corr}) suggests an increased cross-linking density in the paint. In some cases, an induction time (indicated by t_0 and t_{onset}) before oxygen uptake is also observed[2].

Figs. 1 and 2 show the experimental curves normalized for the oil content and those obtained by the fitting according to Eq. (1), and Table 3 displays the curve-fitting parameters along with the χ^2 and R coefficients.

Focusing first on those paints prepared starting from CdS pigments, based on their oxidative behaviour they can be divided into three groups (Fig. 1 and Table 3). The pure cubic and hexagonal forms (CUB and HEX) based paints are in the first group; the W&N series and KP4 fall into the second group, while the Y paint series belongs to the third group.

The first group featuring pure cubic and hexagonal forms CUB and HEX show induction time (t_0 and t_{onset}), amount of oxygen added (C), effective total mass loss values and apparent rate constants (λ_0 and λ_1) very similar to that of linseed oil alone. The induction time values are the lowest among those measured in this study.

W&N series and KP4 paints exhibit longer induction times (t_0 and t_{onset}) and a lower oxygen uptake (C). However, they produce a film with a higher cross-linking density (lower values of A_{corr}) compared to CUB and HEX. W&N6 significantly slows down peroxide formation (λ_0).

The behavior of Y series (Y3, Y5 and Y9) differs most among the paint samples analysed. The experimental data of Y3 could not be fitted, as in 4000 minutes the curve was still incomplete. Overall, the induction time of Y series is significantly longer compared to the other systems (t_0 and t_{onset}). Y5 is characterized by the highest value oxygen added to oil (C).

By considering the curing under TG condition of pigments containing selenium, CdSe paint has similar induction time, takes less oxygen (C) but undergoes similar oxidative degradation (A_{corr}) than CUB and HEX paints. The oxygen uptake curve of $CdS_{(0.72)}Se_{(0.28)}$ paint is different from both CUB, HEX and CdSe paints and it cannot be described as a linear combination of CdSe and HEX paints curves weighted according to the Se/S ratio (Fig. 2). In particular $CdS_{(0.72)}Se_{(0.28)}$ paint presents about three times longer induction time than the theoretical curve, undergoes about three-time less oxidative degradation and it uptakes one third of oxygen. Overall, the induction time is strongly increased when the size of crystallite in nanometric (Y series). Accordingly, unlike the other paints, Y paints - containing pigments with amorphous structures and the smallest crystallite size (3 nm) – were still quite liquid also after 4000 min inside the thermobalance at 80°C, indicating that the curing process was far from complete.

This behaviour cannot be attributed to the photocatalytic activity of the pigment as TGA measurements were carried out in the dark. We hypothesize that CdS pigments could exhibit a peroxidase-like (POD-like) catalytic activity[26,29] in oil, as they do in aqueous solutions. As a result of this activity, peroxides, both alkyl peroxides (ROOR) and hydroperoxides (ROOH), formed within the oil curing can be reduced to their corresponding alcohol (ROH) and water. This reaction pathway effectively terminates oil autoxidation and crosslinking, as it competes with the typical decomposition of peroxides into radical species, which are essential for the propagation of lipid autoxidation. Consequently, the reduction of peroxides delays the onset of radical propagation and extends the induction period prior to the observed mass increase. The mechanism of POD-like activity is still unclear and it has been only partially explained for certain inorganic semiconductors such as FeS_2 and Fe_3S_4, by means of density functional theory calculations[42]. It is reported that this catalytic activity could be related to i) the high surface-to-volume ratio - due to the nanometric dimensions of the catalyst[26]; ii) the presence of the structural defects - such as cadmium or sulphur vacancies which can modulate the pigment interactions with molecular oxygen and water and peroxides[32]; iii) the partial substitutions of Cd^{2+} or S^{2-} with other cations or anions[43–44]. The behaviour $CdS_{(0.72)}Se_{(0.28)}$ could be an example of this specific case as Se partially substitutes S in the crystal.

FTIR spectra of the pigments shows that Y pigments (Fig. S1 in the Supporting Information) have a relative amount of water bound to the pigment structure. The presence of water in these pigments induces a relatively high-water content into the paint composition, as can be seen from the TGA data reported in Fig. 1 (around 0.1 % for HEX paint and around 2.8 % for Y9 paint). In previous studies on ultramarine blue pigment, the presence of water in the pigment(which was kept for 1 month in an environment with 72 % RH) results in a paint water content of around 0.1 %, and this does not affect the induction time of the paint [10]. Conversely, literature studies on the effect of water activity on the autoxidation process of methyl linoleate [45] which can be considered a model oil system, show that the value of the water activity influences the induction period of the autoxidative process. Once a certain amount of water is present in the system, the peroxides/hydroperoxides formed are stabilised by the formation of hydrogen bonds, thus prolonging the induction period. The high water content in the paint with Y pigments could partially account for the delay in the induction time of the resulting paints. In our opinion, the presence of water in the paint cannot account for the extreme delay in oil autoxidation, as a delay is also present in other paints with a very low water content. Furthermore, it cannot explain the peculiar behaviour of $CdS_{(0.72)}Se_{(0.28)}$ compared to CdSe and HEX.

Before and after the TGA, infrared spectra of the paints were acquired to assess changes in the spectral features resulting from oil oxidation during accelerated paint curing conditions (Fig. 3). The spectra before TG analyses are characterized by the distinct signals associated with fresh linseed oil[15].

Differences in the infrared band intensities are visible when comparing the samples before and after thermal ageing that are due to the oil curing. These include reduction in the stretching band of cis (C=C-H) band at 3010 cm^{-1} and an increase in the stretching band of trans (C=C-H) bands at 966 cm^{-1} and 985 cm^{-1} due to double bond isomerization and an increase of the 1633 cm^{-1} band related with the formation of conjugated C=C[46–47]; broadening of the ester νC=O band at 1744 cm^{-1} associated with the formation of oxidized moieties such as carboxylic acids, aldehydes and ketones[47]; a shoulder at 1783 cm^{-1} ascribable to secondary oxidations products containing carbonyl functional groups such as peracids, peresters, lactones and anhydrides [47]. In the HEX based paint, the cis ν(C=C-H) bands (Fig. 3-b) disappear after thermal ageing. In all pains except for the Y series, two distinct shoulders appear at 1720 cm^{-1} and 1783 cm^{-1} highlighting the formation of polar oxidation products and an increased νO-H band at 3400 cm^{-1}, indicative of hydroxyl moieties formation[2] (Fig. 3-a,b,c,d,e,i). IR measures confirmed that in the Y series is characterised by the slowest curing rate.

The reduction of stretching band of cis (C=C-H) and the increase of in the stretching band of trans (C=C-H) bands is used as an indicator of the progress of the early stages of the curing process, and so these data can be compared with the TGA data.

- CUB, HEX: after thermal ageing stretching band of cis (C=C-H) is strongly reduced and completely absent, respectively in agreement with the fastest curing kinetics observed. Moreover these system tend to undergo more oxidative degradation compared to the other pigmented systems.
- W&N1, W&N6, KP4, $CdSe_{(0.28)}S_{(0.72)}$: stretching band of cis (C=C-H) is still present after thermal ageing, in agreement with the slower curing kinetics observed by TGA. The materials appear to undergo less oxidative degradation over time.

Y3, Y5 and Y9 show unique spectral features, including a broad νO-H band at 3400 cm^{-1} due to the presence of water before thermal oxidation (Fig. 3-f, g,h). After thermal oxidation, the band at 3400 cm^{-1} is strongly reduced indicating that water evaporated during thermal treatment at 80°C.The presence of stretching band of cis (C=C-H) at 3010 cm^{-1} confirmed the slower curing process (Fig. 3-f, g,h). Moreover for samples

Table 4
Assignment of the main absorption bands observed in *ATR-FTIR spectra in Fig. 3 (ν = symmetric stretching, δ = bending)* with an indication of which bands were detected in each sample after TGA thermal treatment.

		Identification after thermal ageing								
Absorption band	Assignment	CUB	HEX	W&N1	W&N6	KP4	Y3	Y5	Y9	$CdS_{(0.72)}Se_{(0.28)}$
3500-3300	ν(OH)	✓	✓	✓	✓	✓	✓	✓	✓	✓
3010	ν(C=C), cis configuration			✓	✓	✓	✓	✓	✓	✓
1783	ν(C=O), secondary oxidation products	✓	✓	✓			✓			✓
1744	ν(C=O), esters	✓	✓	✓	✓	✓	✓	✓	✓	✓
1720	ν(C=O), ketons, aldehydes, carboxylic acids	✓	✓	✓	✓	✓	✓	✓	✓	✓
1544	$\nu(COO^-)$, carboxylates				✓	✓	✓	✓	✓	
1465	δ(CH) CH_2, CH_3	✓	✓	✓	✓	✓	✓	✓	✓	✓
1097	$\nu(SO_4^{2-})$					✓	✓	✓	✓	
966	ν(C=C), trans configuration	✓	✓	✓	✓	✓	✓	✓	✓	✓

Y3, Y5, Y9, W&N6 and KP4 (Fig. 3-d,e,f,g,h) the band observed at 1544 cm^{-1} is attributed to symmetric stretching of COO^-, indicating the formation of cadmium soaps within the paint films [48]. Y3, Y5 and Y9 (Fig. 3-f,g,h) are also characterized by a relative increase of the band at 1097 cm^{-1} due to the symmetric stretching of SO_4^{2-} related to the possible formation of $CdSO_4$ or $CdSO_4 \cdot nH_2O$[30]. The POD-like activity in aqueous solution implies that peroxides are reduced and an organic substrate is oxidised. In this oil binder we can consider as viable options both the oxidation of alcoholic functional groups to aldehydic and acidic moieties, as well as sulphur oxidation from S^{2-} to SO_4^{2-}. Table 4 summarises the ATR-FTIR band identification and the indication of the different functional groups detected after thermal ageing in the different paint samples.

4. Conclusions

This study highlights that pigments with same chemical compositions but differing in crystalline proprieties - such as degrees of crystallinity, crystalline forms and crystallite sizes, can significantly influence the curing kinetics, i.e. the induction time before the onset of oil curing, and affect the resulting film chemical characteristics, in terms of its polarity, cross-linking density, and the presence of metal carboxylates and cadmium sulphates. Particularly noteworthy is the behaviour of CdS pigments containing nanocrystals (Y series), which are already linked to degradation phenomena of oil paintings. These nanocrystalline forms markedly inhibit peroxide propagation, delaying the polymer formation, and simultaneously promote cadmium carboxylates and cadmium sulphates formation. Such behaviour suggests the involvement of intrinsic peroxidase-like catalytic activity in oil [26,29], as they do in aqueous solutions, that competes with the typical radical-driven curing process. We hypothesise that this occurs through peroxides and hydroperoxides (ROOR or ROOH) reduction, thus terminating the oil autoxidation and crosslinking. Overall, the findings underscore that pigments with the same nominal chemical formula but differing physical properties can lead to paint films with significantly different molecular features. The preliminary evidence of POD-like activity in CdS pigments presented here warrants further investigation. Future work should expand the sample set to include a broader range of nanocrystalline CdS materials with different crystallite sizes. In addition, it would be valuable to extend the series of CdSSe samples to include varying S/Se ratios.

CRediT authorship contribution statement

Giulia Caroti: Writing – original draft, Methodology, Investigation, Data curation. **Silvia Pizzimenti:** Writing – original draft, Visualization, Supervision, Methodology, Investigation, Data curation, Conceptualization. **Rafaella Georgiou:** Writing – review & editing, Methodology, Investigation. **Marta Ghirardello:** Writing – review & editing, Investigation, Conceptualization. **Rita Carosi:** Writing – review & editing, Investigation. **Emma Cantisani:** Writing – review & editing, Methodology, Investigation. **Ilaria Bonaduce:** Writing – review & editing, Supervision, Resources, Methodology, Conceptualization. **Daniela Comelli:** Writing – review & editing, Supervision, Funding acquisition, Conceptualization. **Celia Duce:** Writing – original draft, Visualization, Supervision, Project administration, Funding acquisition, Conceptualization.

Declaration of competing interest

The authors declare that they have no known competing financial interests or personal relationships that could have appeared to influence the work reported in this paper.

Supplementary materials

Supplementary material associated with this article can be found, in the online version, at doi:10.1016/j.thradv.2026.100096.

Data availability

Data will be made available on request.

References

[1] I. Bonaduce, C. Duce, A. Lluveras-Tenorio, J. Lee, B. Ormsby, A. Burnstock, K.J. van den Berg, Conservation issues of modern oil paintings: A molecular model on paint curing, Acc. Chem. Res. 52 (12) (2019) 3397–3406.
[2] S. Pizzimenti, L. Bernazzani, C. Duce, M.R. Tinè, I. Bonaduce, A versatile method to fingerprint and compare the oxidative behaviour of lipids beyond their oxidative stability, Sci. Rep. 13 (1) (2023) 8094.
[3] S. Pizzimenti, L. Bernazzani, M.R. Tinè, C. Duce, I. Bonaduce, Unravelling the effect of carbon black in the autoxidation mechanism of polyunsaturated oils, J. Therm. Anal. Calorim. 147 (9) (2022) 5451–5462.
[4] S. Pizzimenti, L. Bernazzani, M.R. Tinè, V. Treil, C. Duce, I. Bonaduce, Oxidation and cross-linking in the curing of air-drying artists' oil paints, ACS Appl. Polym. Mater. 3 (4) (2021) 1912–1922.
[5] S. Pizzimenti, G. Caroti, L. Bernazzani, J. La Nasa, E. Pulidori, A.F. Bonatti, C. De Maria, G. Van Assche, F. Martini, M. Geppi, Impact of selected driers on the curing kinetics, thermodynamics, and molecular features of commercial artists' oil paints, J. Cult. Herit. 73 (2025) 465–475.
[6] O. Ranquet, C. Duce, E. Bramanti, P. Dietemann, I. Bonaduce, N. Willenbacher, A holistic view on the role of egg yolk in Old Masters' oil paints, Nat. Commun. 14 (1) (2023) 1534.
[7] M. Li, Y. Li, Y. Zong, Y. Song, Y. Liao, Y. Yang, Y. Zhu, Application of manganese-based driers in tung oil: drying behavior, paint film properties, and drying mechanism, Ind. Crops Prod. 206 (2023) 117733.
[8] S. Kirkpatrick, J. Sanyova, K. Janssens, G. Van der Snickt, The synergistic influence of metal cations on the drying and viscosity of linseed oil assessed by means of model samples containing synthesised metal carboxylates, Herit. Sci. 12 (1) (2024) 209.
[9] F. Modugno, F. Di Gianvincenzo, I. Degano, I.D. van der Werf, I. Bonaduce, K.J. van den Berg, On the influence of relative humidity on the oxidation and hydrolysis of fresh and aged oil paints, Sci. Rep. 9 (1) (2019) 1–16.
[10] G. Caroti, O. Ranquet, S. Pizzimenti, L. Bernazzani, E. Cantisani, R. Punis, A. Zoleo, P. Dietemann, N. Willenbacher, C. Duce, On the preparation of model ultramarine blue oil paint layers: factors affecting the wet paint flow and curing, J. Cult. Herit. 76 (2025) 239–250.
[11] I. Bonaduce, L. Carlyle, M.P. Colombini, C. Duce, C. Ferrari, E. Ribechini, P. Selleri, M.R. Tine, New insights into the ageing of linseed oil paint binder: a qualitative and quantitative analytical study, PLoS One 7 (11) (2012) e49333.

[12] D. Erhardt, C.S. Tumosa, M.F. Mecklenburg, Long-term chemical and physical processes in oil paint films, Stud. Conserv. 50 (2) (2005) 143–150.
[13] Y. Chen, X. Ge, S. Zuo, J. Wang, Effect of drying oil on properties of traditional painted coatings, Coatings 14 (12) (2024) 1545.
[14] L. Baij, J.J. Hermans, K. Keune, P. Iedema, Time-dependent ATR-FTIR spectroscopic studies on fatty acid diffusion and the formation of metal soaps in oil paint model systems, Angew. Chem. Int. Ed. 57 (25) (2018) 7351–7354.
[15] M. Gnemmi, L. Fuster-Lòpez, M. Mecklenburg, A. Murray, S. Sands, G. Watson, F. C. Izzo, Ion migration mechanisms in the early stages of drying and degradation of oil paint films, npj Mater. Degrad. 8 (1) (2024) 63.
[16] S. Pizzimenti, F. Saitta, M. Signorelli, M.R. Tinè, I. Bonaduce, C. Duce, D. Fessas, Oil crystallization properties as an index for monitoring early stage curing of oil-based paints: DSC analysis on linseed oil systems, J. Therm. Anal. Calorim. 147 (19) (2022) 10285–10292.
[17] D. Comelli, D. MacLennan, M. Ghirardello, A. Phenix, C. Schmidt Patterson, H. Khanjian, M. Gross, G. Valentini, K. Trentelman, A. Nevin, Degradation of cadmium yellow paint: new evidence from photoluminescence studies of trap states in Picasso's Femme (Époque des "Demoiselles d'Avignon"), Anal. chem. 91 (5) (2019) 3421–3428.
[18] E. Pouyet, M. Cotte, B. Fayard, M. Salomé, F. Meirer, A. Mehta, E. Uffelman, A. Hull, F. Vanmeert, J. Kieffer, 2D X-ray and FTIR micro-analysis of the degradation of cadmium yellow pigment in paintings of Henri Matisse, Appl. Phys. A 121 (2015) 967–980.
[19] G. Van der Snickt, J. Dik, M. Cotte, K. Janssens, J. Jaroszewicz, W. De Nolf, J. Groenewegen, L. Van der Loeff, Characterization of a degraded cadmium yellow (CdS) pigment in an oil painting by means of synchrotron radiation based X-ray techniques, Anal. Chem. 81 (7) (2009) 2600–2610.
[20] L. Monico, L. Cartechini, F. Rosi, A. Chieli, C. Grazia, S. De Meyer, G. Nuyts, F. Vanmeert, K. Janssens, M. Cotte, Probing the chemistry of CdS paints in the Scream by in situ noninvasive spectroscopies and synchrotron radiation x-ray techniques, Sci. Adv. 6 (20) (2020) eaay3514.
[21] M. Gomez Lobon, M. Ghirardello, E. Juncosa Darder, C. Palomino Cabello, M. Bauza, M. Cotte, A. Burnstock, A. Nevin, S.R. Amato, F.C. Izzo, A study of cadmium yellow paints from Joan Miró's paintings and studio materials preserved at the Fundació Miró Mallorca, Herit. Sci. 11 (1) (2023) 145.
[22] J.L. Mass, R. Opila, B. Buckley, M. Cotte, J. Church, A. Mehta, The photodegradation of cadmium yellow paints in Henri Matisse's Le Bonheur de vivre (1905–1906), Appl. Phys. A 111 (1) (2013) 59–68.
[23] G. Van der Snickt, K. Janssens, J. Dik, W. De Nolf, F. Vanmeert, J. Jaroszewicz, M. Cotte, G. Falkenberg, L. Van der Loeff, Combined use of synchrotron radiation based micro-X-ray fluorescence, micro-X-ray diffraction, micro-X-ray absorption near-edge, and micro-fourier transform infrared spectroscopies for revealing an alternative degradation pathway of the pigment cadmium yellow in a painting by Van Gogh, Anal. chem. 84 (23) (2012) 10221–10228.
[24] Feller, R. L., *Artist's pigments: a handbook of their history and characteristics. Vol. 1*. 1993; Vol. 1.
[25] W. Huckle, G. Swigert, S.E. Wiberley, Cadmium pigments. Structure and composition, Ind. Eng. Chem. Prod. Res. Dev. 5 (4) (1966) 362–366.
[26] S.K. Maji, A.K. Dutta, S. Dutta, D.N. Srivastava, P. Paul, A. Mondal, B. Adhikary, Single-source precursor approach for the preparation of CdS nanoparticles and their photocatalytic and intrinsic peroxidase like activity, Appl. Catal. B: Environ. 126 (2012) 265–274.
[27] L. Zhao, L. Hu, X. Fang, Growth and device application of CdSe nanostructures, Adv. Funct. Mater. 22 (8) (2012) 1551–1566.
[28] L. Jie, X. Gao, X. Cao, S. Wu, X. Long, Q. Ma, J. Su, A review of CdS photocatalytic nanomaterials: morphology, synthesis methods, and applications, Mater. Sci. Semicond. Process. 176 (2024) 108288.
[29] S.K. Maji, A.K. Dutta, D.N. Srivastava, P. Paul, A. Mondal, B. Adhikary, Peroxidase-like behavior, amperometric biosensing of hydrogen peroxide and photocatalytic activity by cadmium sulfide nanoparticles, J. Mol. Catal. A: Chem. 358 (2012) 1–9.
[30] L. Monico, A. Chieli, S. De Meyer, M. Cotte, W. de Nolf, G. Falkenberg, K. Janssens, A. Romani, C. Miliani, Role of the relative humidity and the Cd/Zn stoichiometry in the photooxidation process of cadmium yellows (CdS/Cd1− xZnxS) in oil paintings, Chem.–Eur. J. 24 (45) (2018) 11584–11593.
[31] L. Monico, F. Rosi, R. Vivani, L. Cartechini, K. Janssens, N. Gauquelin, D. Chezganov, J. Verbeeck, M. Cotte, F. d'Acapito, Deeper insights into the photoluminescence properties and (photo) chemical reactivity of cadmium red (CdS1− xSex) paints in renowned twentieth century paintings by state-of-the-art investigations at multiple length scales, Eur. Phys. J. Plus 137 (3) (2022) 1–21.
[32] L. Giacopetti, A. Satta, Reactivity of Cd-yellow pigments: role of surface defects, Microchem. J. 137 (2018) 502–508.
[33] M. Ghirardello, V. Gonzalez, L. Monico, A. Nevin, D. MacLennan, C.S. Patterson, M. Burghammer, M. Réfrégiers, D. Comelli, M. Cotte, Application of synchrotron radiation-based micro-analysis on cadmium yellows in Pablo Picasso's femme, Microsc. Microanal. 28 (5) (2022) 1504–1513.
[34] A. Veamatahau, B. Jiang, T. Seifert, S. Makuta, K. Latham, M. Kanehara, T. Teranishi, Y. Tachibana, Origin of surface trap states in CdS quantum dots: relationship between size dependent photoluminescence and sulfur vacancy trap states, Phys. Chem. Chem. Phys. 17 (4) (2015) 2850–2858.
[35] Levin, B. D.; Finnefrock, A. C.; Hull, A. M.; Thomas, M. G.; Nguyen, K. X.; Holtz, M. E.; Plahter, U.; Grimstad, I.; Mass, J. L.; Muller, D. A., Revealing the nanoparticle composition of Edvard Munch's the Scream, and implications for paint alteration in iconic early 20th century artworks. *arXiv preprint arXiv:1909.01933* 2019.
[36] L. Xu, H.-W. Liang, Y. Yang, S.-H. Yu, Stability and reactivity: positive and negative aspects for nanoparticle processing, Chem. Rev. 118 (7) (2018) 3209–3250.
[37] S. Mayda, L. Monico, D. Krishnan, S. De Meyer, M. Cotte, J. Garrevoet, G. Falkenberg, I.C. Sandu, B. Partoens, D. Lamoen, A combined experimental and computational approach to understanding CdS pigment oxidation in a renowned early 20th century painting, Chem. Mater. 35 (24) (2023) 10403–10415.
[38] R. Mayer, Artist's Handbook of Materials and Techniques: Revised and Updated, Viking Books, 1991.
[39] M. Ghirardello, V. Otero, D. Comelli, L. Toniolo, D. Dellasega, L. Nessi, M. Cantoni, G. Valentini, A. Nevin, M.J. Melo, An investigation into the synthesis of cadmium sulfide pigments for a better understanding of their reactivity in artworks, Dyes Pigments 186 (2021) 108998.
[40] R. Sato, H. Itoh, S. Yamashita, An X-ray diffraction study of precipitated cadmium sulphide, Jpn. J. Appl. Phys. 3 (10) (1964) 626.
[41] M. Short, E. Steward, Measurement of disorder in zinc and cadmium sulphides, Mineralogical Society of America, 1959.
[42] H. Cao, Y. Yuan, R. Zhao, W. Shi, J. Jiang, Y. Gao, L. Chen, L. Gao, Deciphering the catalytic mechanism of peroxidase-like activity of iron sulfide nanozymes, ACS Appl. Mater. Interfaces 16 (24) (2024) 30958–30966.
[43] Z.-Z. Xu, B.-F. Xu, A.P. Tanjung, L. Zhang, A.-J. Wang, P. Song, L.-P. Mei, J.-J. Feng, Bio-inspired MOF nanozyme-engineered biocatalytic precipitation strategy mediates electron transfer for ultrasensitive photoelectrochemical immunoassay, Sens. Actuators B: Chem. 412 (2024) 135732.
[44] H. Wei, E. Wang, Nanomaterials with enzyme-like characteristics (nanozymes): next-generation artificial enzymes, Chem. Soc. Rev. 42 (14) (2013) 6060–6093.
[45] A. Gopala Krishna, J. Prabhakar, Effect of water activity on secondary products formation in autoxidizing methyl linoleate, J. Am. Oil Chem. Soc. 69 (2) (1992) 178–183.
[46] M. Lazzari, O. Chiantore, Drying and oxidative degradation of linseed oil, Polym. Degrad. Stab 65 (2) (1999) 303–313.
[47] L. de Viguerie, P. Payard, E. Portero, P. Walter, M. Cotte, The drying of linseed oil investigated by Fourier transform infrared spectroscopy: historical recipes and influence of lead compounds, Prog. Org. Coat. 93 (2016) 46–60.
[48] F.C. Izzo, M. Kratter, A. Nevin, E. Zendri, A critical review on the analysis of metal soaps in oil paintings, ChemistryOpen 10 (9) (2021) 904–921.